

The DWARF project: Eclipsing binaries - precise clocks to discover exoplanets

T. Pribulla^{1,*}, M. Vaňko¹, M. Ammler - von Eiff², M. Andreev^{3,4}, A. Aslantürk⁵, N. Awadalla⁶, D. Baluďanský⁷, A. Bonanno⁸, H. Božić⁹, G. Catanzaro⁸, L. Çelik^{10,11}, P.E. Christopoulou¹², E. Covino¹³, F. Cusano¹⁴, D. Dimitrov¹⁵, P. Dubovský¹⁶, E.M. Esmer^{10,11}, A. Frasca⁸, Ľ. Hambálek¹, M. Hanna⁶, A. Hanslmeier¹⁷, B. Kalomeni¹⁸, D. P. Kjurkchieva¹⁹, V. Krushevskaja²⁰, I. Kudzej¹⁶, E. Kundra¹, Yu. Kuznetsova²⁰, J.W. Lee²¹, M. Leitzinger¹⁷, G. Maciejewski²², D. Moldovan²³, M.H.M. Morais²⁴, M. Mugrauer²⁵, R. Neuhäuser²⁵, A. Niedzielski²², P. Odert¹⁷, J. Ohlert^{26,27}, İ. Özavcı^{10,11}, A. Papageorgiou¹², Š. Parimucha²⁸, S. Poddaný^{29,30}, A. Pop²³, M. Raetz³¹, S. Raetz²⁵, Ya. Romanyuk⁴, D. Ruždjak⁹, J. Schulz³², H.V. Şenavcı^{10,11}, T. Szalai³³, P. Székely³⁴, D. Sudar⁹, C.T. Tezcan^{10,11}, M.E. Törün^{10,11}, V. Turcu²³, O. Vince³⁵, and M. Zejda³⁵

¹ Astronomical Institute, Slovak Academy of Sciences, 059 60 Tatranská Lomnica, Slovakia

² Thüringer Landessternwarte Tautenburg, Sternwarte 5, 07778 Tautenburg, Germany

³ Terskol Branch of INASAN RAS, 81 Elbrus ave., ap. 33, Tyrnauz, Kabardino-Balkaria Republic, 361623 Russian Federation

⁴ International Centre for Astronomical, Medical and Ecological Research, National Academy of Sciences of Ukraine, 27 Akademika Zabolotnoho St, 03680 Kyiv, Ukraine

⁵ University of Ondokuz Mayıs, Faculty of Science, Dept. of Physics, 55139 Kurupelit-Samsun Turkey

⁶ National Research Institute of Astronomy, and Geophysics, Helwan, Cairo, Egypt

⁷ Roztoky observatory, Slovakia

⁸ INAF, Osservatorio Astrofisico di Catania, via S. Sofia, 78, 95123 Catania, Italy

⁹ Hvar Observatory, Faculty of Geodesy, University of Zagreb, 10000 Zagreb, Croatia

¹⁰ University of Ankara, Faculty of Science, Dept. of Astronomy and Space Sciences, 06100 Tandogan-Ankara, Turkey

¹¹ Institute of Theoretical and Applied Physics (ITAP) 48740 Turunç, Muğla, Turkey

¹² Astronomical Laboratory, Dept. of Physics, University of Patras, 26500 Rio-Patras, Greece

¹³ INAF, Osservatorio Astronomico di Capodimonte, via Moiraniello 16, 80131 Napoli, Italy

¹⁴ Osservatorio Astronomico di Bologna, Via Ranzani 1, 40127 Bologna, Italy

¹⁵ Institute of Astronomy and National Astronomical Observatory, Bulgarian Academy of Sciences, 72 Tsarigradsko Shosse Blvd., 1784 Sofia, Bulgaria

¹⁶ Vihorlat Observatory, Mierova 4, 066 01 Humenné, Slovakia

¹⁷ Institut für Physik, IGAM, Karl-Franzens Universität Graz, Universitätsplatz 5, 8010 Graz, Austria

¹⁸ Dept. of Astronomy and Space Sciences, University of Ege, 35100 Bornova, Izmir, Turkey

¹⁹ Dept. of Physics, Shumen University, 9700 Shumen, Bulgaria

²⁰ Main Astronomical Observatory of National Academy of Sciences of Ukraine, 27 Akademika Zabolotnoho St, 03680 Kyiv, Ukraine

²¹ Korea Astronomy and Space Science Institute (KASI), 776 Daedeokdae-ro, Yuseong-gu, Daejeon 305-348, Korea

²² Toruń Centre for Astronomy, N. Copernicus University, Gagarina 11, 87100, Toruń, Poland

²³ Astronomical Institute of the Romanian Academy, Astronomical Observatory Cluj-Napoca, Str. Ciresilor 19, 400487 Cluj-Napoca, Romania

²⁴ Department of Physics & I3N, University of Aveiro, Campus Universitário de Santiago, 3810-193 Aveiro, Portugal

²⁵ Astrophysikalisches Institut und Universitäts-Sternwarte Jena, Schillergäßchen 2, 07745 Jena, Germany

²⁶ University of Applied Sciences, Wilhelm-Leuschner-Straße 13, 61169 Friedberg, Germany

²⁷ Michael Adrian Observatory, Astronomie Stiftung Trebur, Fichtenstrasse 7, 65468 Trebur, Germany

²⁸ Institute of Physics, Faculty of Natural Sciences, Šafárik University, Košice, Slovakia

²⁹ Astronomical Institute, Faculty of Mathematics and Physics, Charles University Prague, V Holešovičkách 2, 180 00 Prague 8, Czech Republic

³⁰ Štefánik Observatory, Strahovská 205, Prague, Czech Republic

³¹ Private observatory, Stiller Berg 6, 98587 Herges-Hallenberg, Germany

³² Volkssternwarte Kirchheim Arnstaedter Straße 49, 99334 Kirchheim, Germany

³³ Dept. of Optics and Quantum Electronics, University of Szeged, Dóm tér 9, 6720 Szeged, Hungary

³⁴ Dept. of Experimental Physics, University of Szeged, Hungary

³⁵ Astronomical Observatory, Volgina 7, 11060 Belgrade, Serbia

³⁶ Dept. of Theoretical Physics and Astrophysics, Masaryk University, Kotlářská 2, 611 37, Brno, Czech Republic

Received 30 Mar 2012, accepted 11 Nov 2012

Published online later

Key words binaries: eclipsing – extrasolar planets: photometry

1 Introduction

With the continuing discovery of extrasolar planets and an expectation that the majority of solar-type stars reside in binary or multiple systems (Duquennoy & Mayor 1991), planetary formation in binary systems has become an important issue (Lee et al. 2009). In general, we can consider planetary companions to binary stars in two types of hierarchical planet-binary configurations: first "S-type" planets which orbit just one of the stars, with the binary period being much longer than that of the planet; second, "P-type" or circumbinary planets, where the planet simultaneously orbits both stars, and the planetary orbital period is much longer than that of the binary (Mutterspaugh et al. 2007). Simulations show either of above possibilities has a large range of stable configurations (see e.g., Broucke 2001; Pilat-Lohinger & Dvorak 2002; Pilat-Lohinger et al. 2003; Benest 2003). Recent theoretical studies (e.g., Moriwaki & Nakagawa 2004; Quintana & Lissauer 2006; Pierens & Nelson 2008) have predicted that P-type planets can form and survive over long timescales. Characterization of such planets is potentially of great interest because they can lead to a better understanding of the formation and evolution of planetary systems around close binary stars, which can be rather different from the case of single stars. (Lee et al. 2009). Hereafter we will consider the "P-type" or circumbinary planets only.

The detection of circumbinary planets is far from being easy. Three principal techniques are: (i) precise radial-velocity (hereafter RV) measurements to detect the wobble of the binary mass center (Konacki et al. 2009), (ii) photometric detection of transits of the planet(s) across the disks of the components of the inner binary (Doyle et al. 2011), and (iii) timing of the inner binary eclipses (Lee et al. 2009).

The classical RV technique is complicated by the fact that the large RV changes of the binary components mask the small wobble resulting from the circumbinary planet(s). In the case of close binaries, the situation is exacerbated by the tidal spin-up of the components, where the projected rotational velocity ($v \sin i$) often exceeds 100 km s^{-1} (see the DDO close-binary project, Pribulla et al., 2009 and references therein). This makes the RV precision insufficient to detect any systemic velocity changes. In fact, there are hardly any binaries where the systemic-velocity changes revealed a third component (unseen in spectra). The second technique - to detect circumbinary planets searching for transits of a substellar companion across a close binary - requires very long photometric runs with excellent accuracy. Assuming that the orbital planes of the underlying binary and the outer orbit of the substellar body are close to being coplanar, the method should be advantageous for edge-on eclipsing binaries (EBs). Three such systems were found in the Kepler satellite photometry: Kepler-16b (Doyle et al., 2011), Kepler-34b and Kepler-35b (Welsh et al. 2012). The latter two systems were actually identified by eclipse

timing. Even if the substellar component is not transiting the inner binary, it causes timing variations of eclipses of the binary system due to the finite velocity of light (light-time effect, hereafter LITE). The eclipses act as an accurate clock for detecting other objects revolving around the inner binary and to determine their orbital parameters from the *observed* – *calculated* times of minima (O-C) in way similar to the solution of RV curves. The timing technique proved to be the most fruitful in detecting circumbinary planets (see Section 2).

The principal goal of the project DWARF is to detect circumbinary planets and/or substellar companions through the timing analysis of selected close eclipsing binaries.

In this paper, we first summarize previous and/or ongoing searches for timing variability (Section 2) and then describe the target selection criteria for the DWARF project (Section 3). In Section 4 we present the CCD data reduction technique and determination of minima times. The following section describes the modeling of the (O-C) residuals for the observed targets. The telescope network put together for continuous photometric monitoring and follow-up observations is described in Section 6.

2 Previous and ongoing searches of circumbinary exoplanets by timing

The timing technique requires to precisely measure the exact instant of some well-defined and repeating feature of the binary-star light curve (LC). It can be pulse arrival time in pulsar binaries or center of minimum in classical eclipsing binaries¹. The former technique proved to be very sensitive and led to detection of the first extrasolar planetary system (PSR1257+12, Wolszczan & Frail, 1992). The latter method does not require high-end instrumentation. It will be utilized in the present observing project.

Timing of the eclipses in binary stars served as a tool to detect unseen components for several decades (see Pribulla & Rucinski, 2006; Beuermann et al. 2011). Unlike the RV variations, the amplitude of the observed LITE increases with orbital period (see equation 5). The technique is, therefore, sensitive to substellar bodies on long-period orbits. With timing accuracies of about ± 10 s for selected EBs showing sharp eclipses, it should be possible to detect circumbinary planets of $\sim 10 M_J$ in long-period orbits of 10 – 20 yr (Ribas 2006).

In the past two decades, the eclipse timing has been used to infer the existence of multiple low-mass planetary objects to a couple of binaries. Early observations focused at the M-dwarf EB CM Dra (see Table 1) which was a very promising target because of deep and narrow eclipses and low total mass. The existence of a planetary system around CM Dra is still dubious (see Deeg et al. 2008; Ofir 2008). A two-planet system orbiting HW Vir, a short-period EB composed of an sdB and an M dwarf, was found by Lee et al. (2009).

* Corresponding author: e-mail: pribulla@ta3.sk

¹ In principle one could use maxima of pulsations in binary stars with pulsating component(s).

Post-common-envelope systems containing a WD and a main-sequence late-type dwarf enable very precise timing because of short ingress and egress durations. The brightest such system, V471 Tau, shows timing variations indicating the presence of a brown-dwarf companion (see Kundra & Hric, 2011). Recently, circumbinary planets were announced around a couple of post-common-envelope systems: two planets in possible mean-motion resonances around the deeply eclipsing binary NN Ser (Beuermann et al. 2010), two giant planets orbiting UZ For (Potter et al. 2011) and a single planet around DP Leo (Qian et al. 2010), HU Aqr (Qian et al. 2011), and RR Cae (Qian et al. 2012). In the case of HU Aqr Gozdziewski et al. (2012) recently showed that the timing data are more consistent with a single planet orbiting the parent star. The exoplanet encyclopedia² lists (as of April 20, 2012) 11 planetary systems (16 planets/4 multiple planet systems) detected by timing. This, however, includes a planet around the *single* pulsating variable star V391 Peg found by the timing technique (Silvotti et al., 2007).

All previous monitoring of EBs focused to find exoplanets by the timing of minima was mostly carried out by individual research groups and telescopes (e.g., Lee et al. 2009; Beuermann et al. 2011; Qian et al. 2011, 2012). An observing campaign to monitor NN Ser over the first half of 2010 was organized by the Göttingen, McDonald, and Warwick research groups (see Beuermann et al. 2010). The only larger initiative, we are aware of, is the Polish project SOLARIS to detect circumbinary planets in the Southern sky (Konacki et al. 2011). The group is establishing a global network of four 50cm robotic telescopes (Australia, Africa and South America) to collect high-precision, high-cadence LCs of selected Southern binaries. The goal for timing precision should be one second per eclipse³.

Because the timing technique is sensitive to extrasolar planets on long-period orbits, the archival data play an important role. A very useful source of the minima timings is the Krakow database prepared and frequently updated by Prof. Kreiner⁴. The major problem when using published timings is the inhomogeneity of the data mostly caused by different approaches to determine the minima. The original LCs are hard to come by. The situation is exacerbated by many mistakes such as heliocentric correction missing, time shifted by one hour or typos. The minima uncertainties are often missing or underestimated.

The presented project has several advantages compared to other studies. Namely: (i) it is complementary to the competing project SOLARIS covering the Southern hemisphere, (ii) it uses only existing facilities, (iii) unlike other projects it would cover relatively extensive list of targets increasing chance of new detection(s), (iv) it is a unique collaboration of many observatories including well equipped amateurs.

3 Target selection

To get the highest possible accuracy and precision of the eclipse timings necessary to detect exoplanets, we selected objects with sharp and deep minima. The following three groups of objects were included: (i) systems with K or/and M dwarf components (ii) systems with hot subdwarf (sdB or sdO) and K or M dwarf components (iii) post-common-envelope systems with a white dwarf (WD) component. Contact binaries will not be observed within this campaign because of the strong interaction of the components in the common envelope that introduces noise in their light curves. Moreover, their minima are normally broader and the ingress/egress phases less steep than in the previous class of EBs.

In addition to well-studied targets, we will perform follow-up observations of recently discovered detached EBs based on the NSVS data (Hoffman et al., 2008), HAT network data (Hartman et al., 2011) and ASAS data (see Pojmanski, 2002; Pojmanski, 2003, Pojmanski & Maciejewski, 2004ab; Pojmanski et al., 2005).

Because all observatories participating in the campaign are north of the 30th parallel, we limit the objects to systems North of DEC = -10° . To collect as many minima as possible, and to fully cover a minimum within one night from mid-latitudes we excluded objects with orbital periods longer than 5 days. The brightness range of our preliminary sample is $R = 10\text{--}17\text{mag}$, which fits the possibilities of small telescopes with apertures of 20 – 200cm equipped with a low-end CCD camera and at least the *VRI* filter set. Such instrumentation allows us to extend the observing network to well-equipped amateur astronomers. The preliminary target list is given in Table 1.

Chances to discover a circumbinary substellar body depend primarily on three factors: (i) precision and number of the minima which can be achieved; (ii) semi-amplitude of the LITE caused by the body; (iii) intrinsic variability of the binary causing noise in minima timings. The suitability of an object (N_σ in Table 1) can be defined as the peak-to-peak amplitude of LITE caused by such a body, ΔT divided by the theoretical precision of a single minimum timing, Δt , (see the following subsections). Rather arbitrarily we included objects having $\Delta T/\Delta t > 1$.

We consider most advantageous to focus on those binary systems with the richest information concerning their physical and orbital parameters (at least individual masses known). At the same time, we also plan to observe neglected systems to exclude objects with erroneous light-curve classification or identification. For the best candidate eclipsing binaries with missing physical parameters we will strive to obtain dedicated spectroscopy at the Rozhen observatory (Bulgaria) or applying for observing time at major observatories.

3.1 Expected precision of the minima timings

The goal of the project is to determine the times of the minima with the highest possible precision. For the systems

² <http://www.exoplanet.eu/catalog.php>

³ <http://www.projektsolaris.pl/photo/1538.html>

⁴ <http://www.as.up.krakow.pl/ephem/>

Table 1 Target list

Target	α_{2000}	δ_{2000}	M_1 [M_\odot]	M_2 [M_\odot]	Sp.type	A_{OCE} [mag]	ΔT [s]	HJD _I 2 400 000+	Period [days]	d_I [mag]	d_{II} [mag]	D_I [days]	V	R	Δt [s]	N_σ	Ref.
DV Psc	00 13 09.2	+05 35 43	0.49	0.51	K5V+M1V	0.04	4.5	52500.1150	0.30853740	0.32	0.15	0.062	10.6	10.0	1.1	4.1	(1)
PTFEB11.441	00 45 46.0	+41 50 30	0.51	0.35	M3.5+WD		5.0	55438.3165	0.35871000	0.20	0.00			16.3			(2)
NSVS 06507557	01 58 23.9	+25 21 20	0.66	0.28	K9+M3		4.7	54746.3801	0.51508836	0.70	0.23	0.062	13.4	12.6	1.8	2.6	(3)
BX Tri	02 20 50.8	+33 20 48	0.51	0.26	M1V+M4V	0.03	5.4	51352.0616	0.19263590	0.33	0.27	0.072	13.4	12.5	4.2	1.3	(4)
V449 Per	02 57 33.5	+35 14 01						52500.9069	0.94620690					12.5			(5)
GJ 3236	03 37 14.1	+69 10 50	0.38	0.28	M4V	0.02	5.9	54734.9959	0.77126000	0.21	0.19	0.039	14.0	13.5	6.3	0.9	(6)
V912 Per	03 44 32.2	+39 59 35						53287.8523	0.57759120	0.22	0.20			13.1			(9)
NLT11748	03 45 16.8	+17 48 09	0.28	0.27	WD+WD		6.6	55619.4264	0.11601549	0.55	0.11		16.7	16.3			(7)
V471 Tau	03 50 25.0	+17 14 47			K2V+DA			52500.3434	0.52118357	0.03	0.00		9.5	9.5			(8)
HAT-216-0003316	04 40 23.0	+31 26 46			M4V+M5V			54471.3745	2.04813610				15.2	13.3			(9)
AP Tau	04 54 45.0	+26 55 24						52500.1267	0.97197470				13.0				(5)
HAT-131-0026711	05 16 36.9	+48 35 44						54497.1710	0.66395310	0.30	0.10		14.3				(9)
HAT-133-0002525	06 36 25.2	+43 49 47				0.03		53632.4735	1.59457150	0.40	0.16	0.096	13.8		4.8		(9)
V470 Cam	07 10 42.1	+66 55 44	0.48	0.13	sdB+M	0.04	6.3	51822.7598	0.09564665	1.00	0.20	0.015	14.7	14.6	1.2	5.4	(10)
YY Gem	07 34 37.4	+31 52 10	0.60	0.60	dM1e	0.06	4.0	52500.4573	0.81428330	0.55	0.50		10.6	9.1			(11)
HAT-136-0003262	08 11 34.8	+43 02 33						53770.8395	0.64948470	0.60	0.65	0.071	14.3		3.4		(9)
GSC 1941 1746	08 25 51.9	+24 27 04	0.56	0.65	M2V+M2V		4.0	53730.7303	2.26560000	0.90	0.40	0.453	12.9		3.0	1.3	(12)
CU Cnc	08 31 37.6	+19 23 39	0.43	0.40	M5Ve	0.03	5.1	50208.5068	2.77146800	0.13	0.11	0.083	12.1	11.4	6.1	0.8	(13)
NSVS 02502726	08 44 11.0	+54 23 47	0.71	0.35	K5V+M1V	0.04	4.3	54497.5502	0.55975500	0.50	0.35	0.084	14.0	13.4	3.9	1.1	(14)
GSC 2499 246	09 16 12.3	+36 15 34	0.68	0.73	M3V+M3V		3.6	53456.6763	0.36697100	0.90	0.60	0.070	12.5		1.0	3.6	
HAT-225-0003429	09 21 28.4	+33 25 59				0.02		54534.1898	0.42647590	0.28	0.27	0.047	14.5		6.6		(9)
BS Uma	11 25 41.0	+42 34 50			K9-M1V	0.10		52500.3477	0.34950990	0.41	0.35	0.059	12.5	11.5	2.0		(16)
HW Vir	12 44 20.2	-08 40 17	0.48	0.14	sdB+M6-7		6.2	52500.0560	0.11671947	0.80	0.15	0.014	10.5		0.2	31.0	(17)
DE CVn	13 26 53.3	+45 32 47	0.51	0.41	M3V+DA		4.8	52784.5533	0.36413940	0.10	0.00		12.8	12.2			(18)
NY Vir	13 38 48.1	-02 01 49	0.50	0.15	sdB+M5		6.0	52500.0594	0.10101598	0.90	0.15	0.012	13.3	13.5	0.6	10.0	(10)
NSVS 01031772	13 45 34.9	+79 23 48	0.54	0.50	M2V	0.02	4.4	53456.6796	0.36814140	0.60	0.60	0.055	12.6	11.0	0.8	5.2	(19)
HAT-145-0001586	13 45 13.2	+46 18 40				0.01		53843.9266	1.58752710	0.65	0.55	0.064	14.3		3.1		(9)
GK Boo	14 38 20.7	+36 32 25			K2V	0.04		52500.4350	0.47777170	0.92	0.77	0.091	10.6	10.5	0.5		(20)
GU Boo	15 21 54.8	+33 56 09	0.60	0.59	M0/M1.5	0.15	4.0	52723.9811	0.48871000	0.90	0.65	0.064	13.1	12.9	1.2	3.2	(21)
NSVS 07826147	15 33 49.4	+37 59 28	0.38	0.11	sdB+M5		7.2	54524.0195	0.16177042	1.35	0.20	0.016	13.0	13.4	0.4	18.1	(15)
G179-55	15 47 27.4	+45 07 51	0.26	0.26	M4		7.0	51232.8953	3.55001840	0.05	0.06		12.5				(9)
NN Ser	15 52 56.1	+12 54 45	0.54	0.11	DAO1+M4		6.0	52500.1209	0.13008015	>2	0.00		16.7				(22)
HAT-192-0001841	16 12 16.7	+41 13 51				0.02		53853.9056	0.30873570	0.62	0.55	0.037	14.0		2.1		(9)
CM Dra	16 34 20.4	+57 09 44	0.23	0.21	M4.5V	0.03	7.7	52500.7177	1.26839010	0.75	0.60	0.038	12.9	10.9	9.9	0.8	(23)
TrES-Her0-07621	16 50 20.7	+46 39 01	0.49	0.49	M3V+M3V		4.6	53139.7495	1.12079000	0.11	0.10	0.090	15.5		36.8	0.1	(24)
HAT-196-0006238	17 58 59.3	+35 55 12						53623.7449	1.75834310				14.9				(9)
V924 Oph	18 33 28.3	+07 07 51							0.35955400					12.9			(5)
OT Lyr	19 08 10.0	+29 13 42						54222.4568	0.47109500					14.1			(5)
FP Sge	20 14 45.8	+19 36 49						52500.2947	0.64200717					14.0			(5)
NSVS 14256825	20 20 00.4	+04 37 56	0.46	0.21	sdO+M2		5.9	51288.9198	0.11037410	0.75	0.20	0.014	13.2	13.3	0.7	7.9	(25)
FI Del	20 29 16.0	+14 45 59						52500.3	0.41592810					14.6			(5)
MR Del	20 31 13.5	+05 13 08	0.69	0.63	K0V	0.01	3.7	52500.3087	0.52169040	0.33	0.17	0.073	11.0	8.9	1.4	2.7	(26)
RX J2130.6+4710	21 30 18.5	+47 10 07	0.55	0.55	M4V+WD		4.2	52785.6819	0.52103563	>2	0.00		13.0				(27)
HS 2231+2441	22 34 21.5	+24 56 57	0.30	0.30	sdB+dM		6.3		0.11058798				14.0	14.0			(28)
HAT-205-0007777	22 42 07.5	+39 02 44						53146.0021	1.11001010				14.6				(9)

Explanation of columns: α_{2000} , δ_{2000} - equatorial coordinates given for epoch and equinox 2000.0; $M_{1,2}$ - masses of the components; spectral classification; A_{OCE} - observed O'Connell effect amplitude expressed as difference in maxima levels; ΔT - amplitude of the LITE for 1 Jupiter mass planet orbiting the binary on 10 years orbit; HJD_I, Period - ephemeris for the primary (deeper) minimum; d_I , d_{II} - minima depth for the *I* passband (for the *V* passband typed in italics); D_I - duration of the primary eclipse; V , R - out-of-eclipse brightness of the binary; Δt - theoretically achievable minimum precision using a 60cm telescope (equation 4) for the primary minima; $N_\sigma = \Delta T/\Delta t$ detection sensitivity of the binary.

References: (1) Zhang, Zhang & Zhu (2010), (2) Law et al. (2012), (3) Cakirli & İbanoğlu (2010), (4) Dimitrov & Kjurkchieva (2010), (5) Malkov et al. (2006), (6) Irwin et al. (2009), (7) Parsons et al. (2011), (8) Kundra & Hric (2011), (9) Hartman et al. (2011), (10) Camurdan et al. (2012), (11) Torres & Ribas (2002), (12) unknown, (13) Ribas (2003), (14) Cakirli et al. (2009), (15) For et al. (2010), (16) Wils et al. (2010), (17) Lee et al. (2009), (18) van den Besselaar et al. (2007), (19) López-Morales et al. (2006), (20) Zasche et al. (2012), (21) Windmiller et al. (2010), (22) Parsons et al. (2010), (23) Morales et al. (2009), (24) Creevey et al. (2005), (25) Wils et al. (2007), (26) Djurašević et al. (2011), (27) Maxted et al. (2004), (28) Ostensen et al. (2008)

with triangular shape of the minima (i.e., binaries with partial eclipses and non-degenerate components⁵) the brightness uncertainty (in magnitudes) of a single observational point, σ , is clearly related to its time uncertainty, δt by the slope of the minimum branch. Then the minimum uncertainty, Δt , can be estimated as:

$$\Delta t = \frac{D\sigma}{2d\sqrt{N}}, \quad (1)$$

⁵ In the case of eclipses of degenerate components, where egress and ingress last typically from couple of seconds to a minute, the time resolution of the photometry defines the timing precision.

where d is the depth (in magnitudes) and D duration of the minimum, and N number of observational points during the eclipse. The above relation shows that the precision of the minimum time increases with the number of datapoints taken in the minimum and their precision, which mostly relates to the diameter of the telescope. The shape of minimum also affects the precision of the timing - deep and at the same time narrow minima provide the best precision⁶.

⁶ Doyle et al. (1998) suggested exact but substantially more complicated approach taking into account exact shape of the minimum and sampling of the observations.

The expected precision of the minima (as given by the shot noise) clearly depends on the size of the telescope and exposure time. Uncertainty of an individual observing point is inversely proportional to the product of collecting area of the telescope and exposure time, E (assuming no read-out nor scintillation noise). If A is the aperture or the diameter of the telescope used, then:

$$\sigma \propto \frac{1}{\sqrt{\pi \left(\frac{A}{2}\right)^2 E}}. \quad (2)$$

Assuming no read-out overheads (then $N = D/E$) combining (1) and (2) one can find that:

$$\Delta t = C \frac{\sqrt{D}}{\sqrt{\pi} A d}. \quad (3)$$

Proportionality factor, C , can be quantified counting the photons coming from the source taking into account the telescope throughput, filter transparency, quantum efficiency of the detector and atmospheric extinction. If the average brightness of the target during the eclipse is m_λ , and it is observed at the air mass X at (the wavelength-dependent) extinction coefficient κ_λ then (see Sections 1.7, 1.8 and 2.5 of Henden & Kaitchuck, 1982):

$$\Delta t = \frac{1}{\sqrt{\tau F_\lambda}} 10^{0.2(m_\lambda + X \kappa_\lambda)} \frac{\sqrt{D}}{\sqrt{\pi} A d}. \quad (4)$$

The constant τ is the throughput of the observing system⁷, and F_λ is number of photons from a $m_\lambda = 0$ star per square meter and second outside Earth atmosphere recorded through the filter used. Preliminary observations from the 60-cm telescope equipped with the MI G4-9000 CCD camera at Stará Lesná show that from a $R = 14$ -mag star, we record 250 photons in one second in the R passband at air mass $X = 1$ and $\kappa_R = 0.2$, which translates to $\tau \approx 0.16$.

Because of several other sources of the noise and non-negligible read-out times (8 sec in the case of the 2x2 binning read-out with the MI G4-9000 CCD camera) the minima uncertainties as estimated by relation (4) and listed in Table 1 should be regarded as the theoretical limits. The estimates, nevertheless, immediately show the suitability of the selected targets for the present project.

3.2 LITE amplitude

It can easily be shown that the full amplitude (Max - Min or peak-to-peak) of the expected LITE changes caused by another body orbiting a binary on the edge-on ($i \sim 90^\circ$) circular orbit ($e \sim 0$) is:

$$\Delta T \approx \frac{2M_3 G^{1/3}}{c} \left[\frac{P_3}{2\pi(M_1 + M_2)} \right]^{2/3}, \quad (5)$$

where M_1, M_2, M_3 are masses of the components, G is gravitational constant, c is speed of light, and P_3 is orbital

period of the third (substellar) component. Eqn. 5 shows that the semi-amplitude of the LITE changes is proportional to the mass of the third component and nearly proportional to its orbital period. The total mass of the underlying binary is also important: having 8 times more massive inner binary decreases the LITE amplitude four times. The advantage of low-mass binaries is, on the other hand, offset by their surface activity causing noise or spurious periodicities in the timing data.

Table 1 quotes, whenever $M_1 + M_2$ is available, the estimated full amplitude, ΔT , in the case of a Jupiter-mass planet orbiting the EB in 10 years. The full (peak-to-peak) amplitude ranges between 4 and 8 seconds. Detecting a Jupiter-mass planet on a shorter orbit is, probably, beyond the expected precision of the timing data: shortening the planet's orbital period 8 times to 1.5 years, would decrease the full amplitude four times to about 1-2 seconds for our targets.

3.3 Intrinsic variability of the binary star

In addition to the timing errors caused by precision and accuracy of the data acquisition, the minima times are affected by intrinsic variability of the binaries. The dominant cause of the intrinsic variability (and enhanced scatter) in the (O-C) diagrams are spots on the active late-type K or M dwarf components. The level of the activity is the highest in the tidally bound close binaries, where magnetic braking could not slow down the rotation. This is the case for systems with orbital periods shorter than about 0.5-1 day. The level of the activity and its effect on the timing varies from system to system. In the most active systems the amplitude of the photometric variations reaches 0.2-0.3 mag (e.g. in DK CVn, Terrell et al., 2005).

Dark photospheric spots seen in the majority of the late-type systems cause LC asymmetries (O'Connell effect) and out-of-eclipse photometric wave(s). A spot seen by the observer close to or during the minimum of light shifts it from the spectroscopic conjunction. A single dark/hot spot not eclipsed during the minimum causes a small linear trend across it. This shifts the observed instant of the minimum from the spectroscopic conjunction. If the maximum following the primary minimum is the brighter/fainter one, then the observed instant of minimum is observed earlier/later than the instant of the spectroscopic conjunction.

The maximum time shift caused by a single starspot can be estimated as follows:

$$\Delta t = \frac{2A_{OCE} D^2}{dP}, \quad (6)$$

where A_{OCE} is observed⁸ peak-to-peak amplitude (see Table 1) of the out-of-eclipse photometric wave, D is the duration of minimum, P is the orbital period, and d is the depth of eclipse. The equation shows that the effect of spots is proportional to the photometric wave amplitude while inversely proportional to the depth of minima. The magnitude

⁷ $\tau \in (0, 1)$ depends on the quantum efficiency of the CCD chip, the absolute transparency of the filter used, the reflection losses on the telescope mirrors etc.

⁸ Most easily estimated as the maxima difference.

of the shift also depends on the method used to determine the minimum instant.

To check for the spot effects which might shift the minimum time from the spectroscopic conjunction, it is advisable to cover parts of the LC just before ingress and just after the egress from the minimum. The difference in the shoulders levels indicates the amplitude of the photometric wave. Another indicator of a spurious shift caused by surface maculation is the minimum asymmetry. This can be checked by the minimum bisectors slant (similar to a technique used in RV exoplanet searches). The bisector method provides best minimum instant estimate as well as realistic errors (see Covino et al., 2004).

When a single photospheric spot causes a trend across the minimum its effect can be rectified using the fitting formula (7) which will be discussed in the following section. The presence of several spots or spots being eclipsed during the minimum complicates the rectification of the effect. The maximum O'Connell effect is listed in Table 1 as OCE. It is pertinent to the *I* passband LC.

Binaries composed of a hot sdB primary and a M dwarf secondary do not show pronounced (>0.02 mag) LC asymmetries. This results from the dominant contribution of the hot subdwarf to the total light of the system. The secondary minimum occurs just due to the eclipse of the irradiated hemisphere of the secondary by the hot subdwarf⁹.

Pulsations of the sdB components, in e.g. NY Vir, pose less serious complication. With the pulsation amplitude not exceeding 0.01 mag and the minimum depth of 0.5–1 mag the shift of the minimum is negligible (see Kilkenney, 2011). To exclude multi-periodic variability of the studied EBs a detailed period analysis of each object will be performed prior to the determination of the minima times. In the case of the positive detection of pulsational variability the LCs will be iteratively pre-whitened.

4 Data reduction process

4.1 CCD frames reduction

The reduction of the CCD frames and aperture photometry will be done using scripts written under the IRAF package¹⁰. The same scripts and approach will be used at all participating institutions.

In the first step, the master dark and flat-field frames will be produced for all exposure times, filters and CCD temperatures. To reduce effects of scattered light usually seen in sky flatfields the master flat fields will be box-car average divided to remove low-frequency variations while pixel-to-pixel sensitivity differences will be preserved. The illumination effects due to vignetting of the CCD chip will be minimized by keeping the EB and its comparison star(s)

at approximately the same pixel coordinates (most of the instruments are autoguided).

In the next step, the raw CCD frames will be dark and flatfield corrected. Then the WCS system will be determined using the GSC 2.3.3 online catalogue for reference¹¹. Finally, aperture photometry of the target and all stars with a brightness within ± 1 mag off target brightness will be performed. The instrumental magnitudes will be determined for several apertures appropriate for the seeing range at the site. All data of a given target from one instrument would be analyzed at the same time to see variability of *all* measured stars on the frames and to select all stable stars to produce an artificial comparison star (see e.g., Broeg et al., 2005).

The resulting LCs will be available on the DWARF project pages¹² for subsequent LC analysis (e.g., determination of photometric elements or detection of pulsations, flares) or redetermination of the minima times.

There are two major systematic complications which can cause spurious shifts in the minima timing: (i) shutter effect during short exposures (ii) non-linearity effects. While the former complication caused by finite speed of the shutter opening can be avoided by using a nearby comparison and avoiding exposures below 10 seconds, the latter effect is harder to quantify. The non-linearity effect, fortunately, does not affect the timing in the case of symmetric minima but can reach a few per cent even well below saturation levels.

4.2 Reference time for the data

Because the goal of the project is going to be accomplished by the accurate (at a level of a few seconds) timing of the LC extrema (in our case minima), it is crucial to regularly synchronize the computer clock with the ntp servers to provide the system time within 1 second off the UTC. Another systematic time shift is connected with the shutter delay: the FITS header gives the instant when the imaging started but it takes a few tenths of a second for the shutter to fully open. This effect will have to be quantified to avoid systematic minima shifts.¹³

UTC (or Coordinated Universal Time) is based on the atomic clocks but it is never allowed to differ from UT1 (based on the rotation of Earth) by more than 0.9 seconds. Therefore a leap second has to be included from time to time (next on June 30, 2012). The UTC, therefore, is discontinuous and not the best to use in timing analysis. It is fully correct to use Barycentric Dynamical Time (TDB) which takes into account relativity – the fact that moving clocks tick at different rates. TDB is a truly uniform time, as we would measure it on Earth if it were not moving around the Sun or being pulled by the Moon and other celestial bodies.

⁹ The true light contribution of the secondary can be seen from the difference in the level of shoulders and that of the mid secondary eclipse, see Fig. 1.

¹⁰ <http://iraf.noao.edu/>

¹¹ <http://gss.stsci.edu/webservices/GSC2/GSC2WebForm.aspx>

¹² <http://www.ta3.sk/~pribulla/Dwarfs/>

¹³ Tests at Astronomical Station Vidojevica/Serbia show that the shutter delay of Alta Apogee E47 CCD camera amount to 0.42 sec.

Using HJD (Heliocentric Julian Date) correction is also not sufficient: the mass center of the Sun revolves around the Solar system barycenter. This causes errors which can reach up to 4 seconds (mostly defined by the orbits of Jupiter and Saturn). Therefore it is best to relate time to the Solar System Barycenter.

Hence we will use Barycentric Julian Dates in Barycentric Dynamical Time (BJD-TDB)¹⁴.

To allow for possible corrections or improvements of UTC to BJD-TDB we will also list times of minima in JD based on UTC (without HJD or BJD correction added).

4.3 Minima determination

The most widespread approach to obtain instants of minima of EBs is to use the Kwee & van Woerden (1956) method. From our experience, the errors estimated using their formula (14) are often unrealistically small. The real uncertainties are often dominated by systematic errors.

The LCs are affected (at the 0.01 mag level) by the red noise (spurious shifts and trends) caused mostly by the atmosphere transparency changes, lack of autoguiding in some of the telescopes and the second-order extinction (Forbes effect). The last effect causes photometry errors even at the same air mass because of differences of spectral types of the target and comparison star(s) (see e.g., Pakstiene & Solheim, 2003). The second-order extinction will be not negligible especially for EBs of very late spectral type when no appropriate comparison star would be found in the field.

To reduce effects of scattered light on sky-flats (centers are most illuminated usually) a box-car averaging will be used (see Section 4.1 and Freundling et al., 2007). This would minimize night-to-night offsets of the LCs.

Our photometry could possibly be improved by using the algorithm based on principal component analysis proposed by Tamuz, Mazeh & Zucker (2005). Unfortunately, the CCD frames will be obtained at several observatories with different setups and even different orientation of the field. Systematic errors in minima positions would be partially removed by the fitting technique proposed below.

For each EB, the fitting templates will be prepared to obtain the instant of conjunction (minimum) for any sufficiently long photometric sequence. Such a way, we will use not only the minima but also other LC segments where the brightness sufficiently changes. The template LC will be produced as the average obtained over the whole campaign.

For EBs with components of widely different temperatures (e.g., sdB + dM systems, or WD + K systems) the amplitude and (relative) depth of minima strongly depends on the wavelength of the observation. Due to the differences in filter transparencies and wavelength response of detectors, we will form a template LC for each filter separately and the fitting LC will be scaled to match the observations.

¹⁴ BJD-TDB differs from the BJD in Coordinated Universal Time (BJD-UTC) by a systematic $32.184 + N$ seconds, where N is the number of leap seconds that have elapsed since 1961 ($N = 34$ as of Jan 1st, 2009).

From our former observing experience, we could also note small nightly shifts of the LCs observed even with the same instrument. Sometimes the LC shows slight but systematic slopes. These slopes are, very probably, caused by scattered light combined with drifting of the targets on the CCD due to imperfect tracking of the telescope.

To obtain good fits of the template $T(x)$ to the observed LCs (and accurate timings), we constructed the following fitting function (see Pribulla et al. 2008):

$$F(x) = A + Bx + CT(x - D), \quad (7)$$

which would allow for shifting, scaling and 'slanting' of the template LC. Fixing of the parameters will be judged according to the appearance of individual LCs, e.g. in the case that only one branch was observed the vertical shift (A) would be fixed to zero.

4.4 Minima uncertainties

As we discussed above, the errors estimated using the classical method for minima determination are usually unrealistically small. To get more realistic estimates and to see the correlations of the parameters, Monte Carlo simulations will be used. To preserve the original shape and scatter of the data, the fitting function $F(x)$ in the instants of real observations will be replicated adding the Gaussian-distributed random noise. The standard deviation of the added noise will correspond to the standard deviation of the original data with respect to the original fit. Preliminary tests show that about 2000 replications of the LC are sufficient to arrive at the errors¹⁵ and correlations of the parameters.

We also considered the bootstrapping of the data (see Press et al. 1993; Efron & Tibshirani, 1993). Because of the small number of datapoints on branches (especially for short-period and WD systems) the randomly re-sampled LCs could skip the crucial phases defining the minimum time and its precision.

5 The timing analysis and its limitations

If an unseen third component revolves an EB, the residuals with respect to a linear (or quadratic) ephemeris will show wavelike behavior in the (O-C) diagram because of the LITE.

Although all our targets are well detached systems (where the mass transfer cannot occur), the orbital period can continuously decrease for two reasons (i) the magnetic braking in the case of systems with late-type components (ii) radiation of gravity waves in the case of the systems with shortest orbital periods (< 0.1 day).

(O-C) curve (due only to the inner binary) can be described by a linear (constant period) or quadratic ephemeris (linear period variation) and if a third body is orbiting the

¹⁵ The standard deviation of given parameters will be determined from the width of its Gaussian distribution profile.

inner binary adding the LITE effect, the times of the minima can be computed as follows:

$$\text{Min } I = JD_0 + P \times E + Q \times E^2 + \frac{a_{12} \sin i}{c} \left[\frac{1 - e^2}{1 + e \cos \nu} \sin(\nu + \omega) + e \sin \omega \right], \quad (8)$$

where $a_{12} \sin i$ is the projected semi-major axis (inclination cannot be derived from the LITE alone), e is the eccentricity, ω is the longitude of the periastron, ν is the true anomaly of the EB orbit around the common center of the mass of the whole system. $JD_0 + P \times E + Q \times E^2$ is the quadratic ephemeris of the minima of the EB and c is the velocity of light. The parameter Q is the coefficient of the quadratic term and gives the rate of the orbital period change of the EB. If a is the semi-major axis of the third (substellar) companion's orbit around the binary's mass center, then:

$$a_{12} = \frac{a M_3}{M_1 + M_2 + M_3}. \quad (9)$$

To obtain the optimal fit and corresponding elements (JD_0 , P , Q , $a \sin i$, e , ω , and also epoch of periastron passage, T_0 , and the period of the orbit of three-body system, P_3) of the LITE orbit including errors, we use the differential corrections method (see Irwin 1959).

The orbital elements determined above enable to estimate the mass of the unseen companion. In the case we know the masses of the binary star components M_1 , M_2 (or their sum), we can derive the mass function of the third-body:

$$\begin{aligned} f(M_3) &= \frac{(M_3 \sin i)^3}{(M_1 + M_2 + M_3)^2} = \\ &= \frac{4\pi^2 (a_{12} \sin i)^3}{G P_3^2} = \frac{4\pi^2 A^3 c^3}{G P_3^2} \end{aligned} \quad (10)$$

where A is the semi-amplitude of LITE (in time units), i is the inclination of the orbital plane of the third body, M_1 , M_2 are the masses of the eclipsing binary components, and M_3 is the mass of the third (substellar) companion, P_3 is the outer orbital period, and G is the gravitational constant.

Assuming that the mass of the substellar body is negligible compared to the total mass of the binary, $M_3 \ll M_1 + M_2$, its mass can be directly found as:

$$M_3^3 \sin^3 i \approx \frac{4\pi^2 (M_1 + M_2)^2}{G P_3^2} A^3 c^3 \quad (11)$$

The analysis of the selected EBs timings will be performed in three steps: (i) period search in the (O-C) residuals with respect to a linear or quadratic ephemeris, (ii) fitting LITE orbits to most promising orbital periods. Orbital periods longer than the time span of the data will not be considered. A major problem in the timing analysis is matching our uncertainties with those listed for the published timings. Moreover, the minima uncertainties are often not given. This will complicate the relative weighting

of the datapoints and cause additional uncertainty of the results.

In the case of K or M dwarf systems both primary and secondary minima would be used. There is no system in our sample showing elliptic orbit. Hence, both types of minima can be simultaneously analyzed. Eventually, we can check the results of the (O-C) curves obtained with primary and secondary minima only before merging both times of minima in a unique curve.

The observed cyclic variations can also be caused by the magnetic-orbital moment coupling mechanism of Applegate (1992). The mechanism causes periodic variations of the orbital period, out-of-eclipse brightness and color. The brightness, color and period changes show the same periodicity. This fact can be used to tell apart the LITE from Applegate's mechanism.

6 Observing network and first observations

The targets will be observed at several observatories using 35-120cm telescopes equipped mostly with low-end CCD cameras (see Table 2). All observatories are in the Northern hemisphere. Hence we limit our targets to those north of $\text{DEC} = -10^\circ$. The longitude spread of the observatories is much larger. This is important because of several EBs with orbital periods longer than one day and for the systems with orbital period being close to integer multiple of one day (e.g., AP Tau or HAT-216-0003316).

To get the best S/N it is advisable to use the R or I filter for M or K EBs (see Section 3), and the V filter (or B in the case of back-illuminated CCDs) for the systems with sdB or WD components¹⁶. Several faint or short-period objects will be observed without filter to provide more light. Using two or more filters would decrease the cadency of the photometry and decrease the duty-cycle because of filter change overheads (this is the case for simple CCD cameras which do not enable simultaneous observing in several passbands). For short-period systems it is advisable to cover both minima shoulders to see the LC asymmetry caused by the photospheric spots.

For most binaries with M and K dwarf components both minima (primary and secondary) are useful for the timing analysis. In the case of sdB EBs or systems with a WD component only the primary minimum will be observed. The secondary eclipse is too shallow (or hardly to be detected) to provide sufficient timing precision in most of those systems.

In addition to the observations focused on the exact timing, we will perform (much less extensive) multi-color $UBVR$ photometry of the same fields to find the best comparison stars (to minimize the second-order extinction effects). The observations will also be focused to check possible out-of-eclipse and color brightness variations which would indi-

¹⁶ The eclipse depth in WD systems is quickly increasing to the shorter wavelength range.

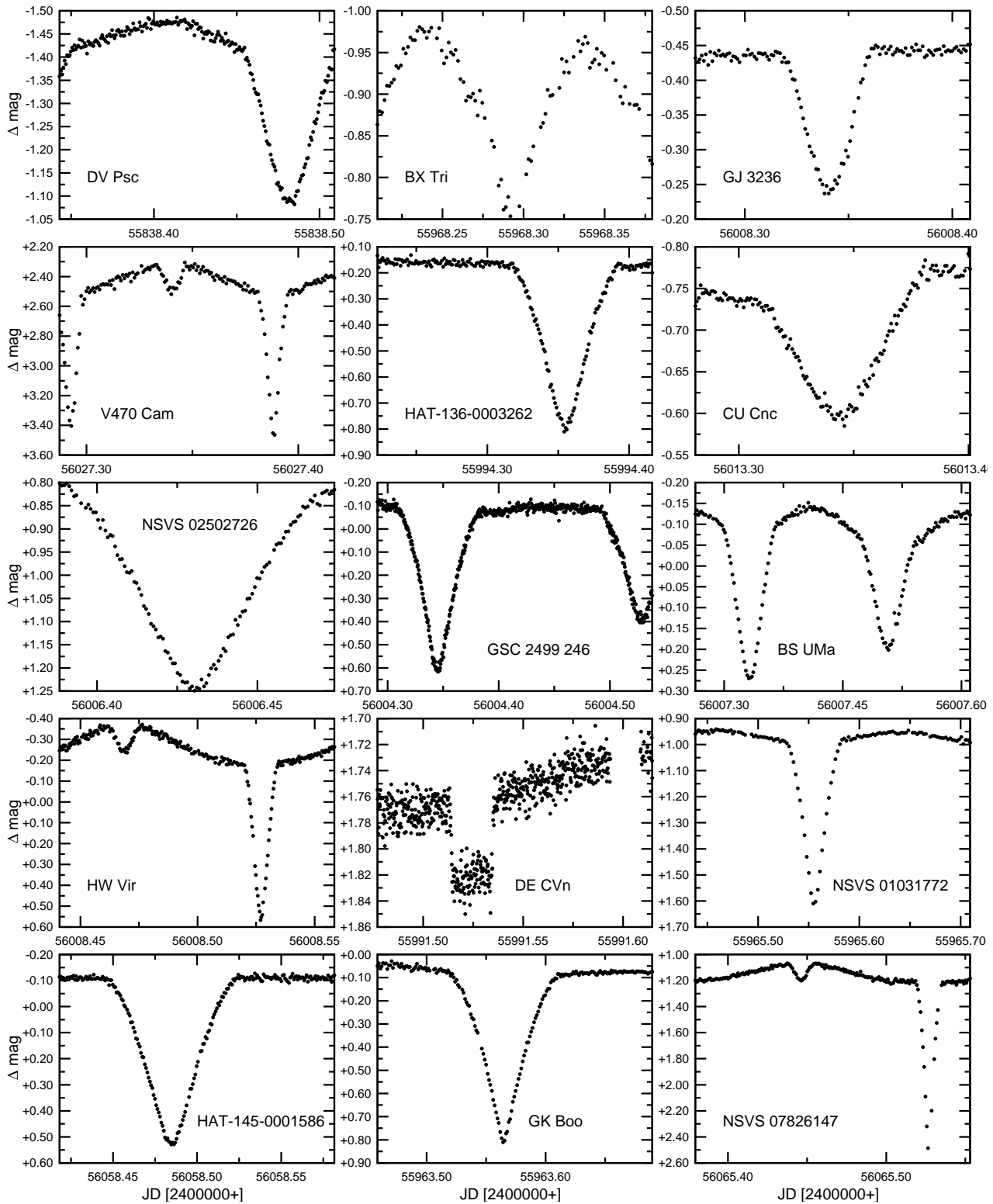


Fig. 1 A sample of LCs obtained at the Stará Lesná observatory using either 50cm Newtonian or 60cm Cassegrain telescopes. The Julian dates are geocentric. LCs of most objects were obtained in the *I* passband (except V470 Cam, HW Vir, DE CVn and NSVS 07826147 observed in the *V* passband).

Table 2 Telescope network (status as of April 22, 2012)

Observatory	Long. [deg.]	Lat. [deg.]	Telescope	Aperture [cm]	Camera	CCD size	FoV [arcmin]	Ref.
SOAO/Korea	128.4E	36.9N	Cassegrain	60	E2V CCD42-40	2048 × 2048	18 × 18	(1)
Terskol/Russia	42.5E	43.3N	Cassegrain	60	Pixel Vision	1024 × 1024	10 × 10	
			Schmidt-Cass.	35	SBIG STL-1001	1024 × 1024	24 × 24	
			Schmidt-Cass.	29	S3C	1024 × 1024	28 × 28	
			Schmidt-Cass.	35	STL-4020M	2048 × 2048	15 × 15	
OMU/Turkey	36.2E	41.4N	Schmidt-Cass.	35	Apogee Alta U-47	1024 × 1024	11 × 11	(2)
Ankara/Turkey	32.8E	39.8N	Schmidt-Cass.	40	Apogee Alta U-47	1024 × 1024	11 × 11	(2)
Kottamia/Egypt	31.8E	29.9N	Cassegrain	188	EEV CCD 42-40	2048 × 2048	2.7 × 2.7	(3)
MAO NASU/Ukraine	30.5E	50.4N	Cassegrain	70	SBIG STL-1001	1024 × 1024	24 × 24	
Lesniki/Ukraine	30.5E	50.3N	Schmidt-Cass.	35	Rolera MGi	512 × 512	7 × 7	
ITAP/Turkey	28.3E	36.7N	Schmidt-Cass.	35	SBIG ST10 XME	2184 × 1472	14 × 10	(4)
Ege/Turkey	27.1E	38.4N	Schmidt-Cass.	40	Apogee CCD47-10	2048 × 2048	20 × 20	(5)
Rozhen/Bulgaria	24.7E	41.7N	Cassegrain	60	FLI ProLine 09000	3056 × 3056	17 × 17	(6)
			Schmidt	50/70	FLI ProLine 16803	4096 × 4096	73 × 73	
			Rit.-Chret.	200	Vers Array 1300B	1340 × 1300	5.7 × 5.7	
Feleacu/Romania	23.6E	46.7N	Schmidt-Cass.	40	SBIG STL-6303E	3072 × 2048	23 × 16	(7)
Kolonica Slovakia	22.3E	48.9N	Cassegrain	100	FLI PL1001E	1024 × 1024	10 × 10	(8)
			Schmidt-Cass.	35	MI G2-1600	1536 × 1024	12 × 8	
			Schmidt-Cass.	50	MI G4-16000	4096 × 4096	31 × 31	
Patras/Greece	21.7E	38.3N	Schmidt-Cass.	35	SBIG ST10 XME	2184 × 1472	20 × 14	
Astron. Station Vidojevica	21.5E	43.1N	Cassegrain	60	Apogee Alta U-42	2048 × 2048	16 × 16	(9)
Serbia			Cassegrain	60	Apogee Alta U-47	1024 × 1024	7.6 × 7.6	(10)
Roztoky/Slovakia	21.5E	49.4N	Cassegrain	40	MI G2-1600	1536 × 1024	12 × 8	
Stará Lesná	20.3E	49.2N	Newton	50	SBIG ST10 XME	2184 × 1472	20 × 14	(11)
Slovakia			Cassegrain	60	MI G4-9000	3056 × 3056	17 × 17	
Szeged/Hungary	20.2E	46.2N	Newton	40	SBIG ST7	765 × 510	17 × 11	
Toruń/Poland	18.6E	53.1N	Cassegrain	60	SBIG STL-1001	1024 × 1024	12 × 12	
Brno/Czech Rep.	16.6E	49.2N	Newton	62	SBIG ST8	1530 × 1020	17 × 11	
			Schmidt-Cass.	35	G2-4000	2056 × 2062		
Hvar/Croatia	16.4E	43.2N	Cassegrain	100	Apogee Alta U-47	2048 × 2048	8 × 8	(12)
Graz/Austria	15.5E	47.1N	Astro_Topar	30	SBIG STL11000M	4008 × 2672	16 × 11	
			Cassegrain	50	SBIG ST-2000XM	1600 × 1200	9 × 7	
			Cassegrain	91	KAF1001E	1024 × 1024	12.5 × 12.5	(13)
Catania/Italy	15.0E	37.7N	Rit.-Chret.	80	Apogee U9000	3040 × 3040	17 (diameter)	(14)
Prague/Czech Rep.	14.4E	50.1N	Schmidt-Cass.	40	SBIG ST10 XME	2184 × 1472	24 × 16	(15)
TLS/Germany	11.7E	51.0N	Schmidt	30	Apogee AP-16	4096 × 4096	132 × 132	(16)
Jena	11.5E	50.9N	Schmidt	60/90	E2V CCD42-10	2048 × 2048	53 × 53	(17)
Germany			Cassegrain	25	E2V CCD47-10	1056 × 1027	21 × 20	(18)
Kirchheim/Germany	11.0E	50.9N	Rit.-Chret.	60	SBIG STL-6303E	3072 × 2048	71 × 52	(19)
Herges-Hallenberg/Germany	10.6E	50.7N	Cassegrain	20	MI G2-1600	1536 × 1024	48 × 32	(20)
Trebur/Germany	8.4E	49.9N	Cassegrain	120	SBIG STL-6303E	3072 × 2048	10 × 7	(21)
LOAO/USA	110.7W	32.4N	Cassegrain	100	ARC 4K CCD	4096 × 4096	28 × 28	(22)

Notes: (1) Lee, Kim & Koch (2007); (2) <http://rasathane.ankara.edu.tr/en/tools.info.php?id=2>; (3) field of view given in the Cassegrain focus, see Azzam et al. (2010); (4) <http://itap-tthv.org/astro/gozlemevi.html>; (5) <http://astronomy.sci.ege.edu.tr/ASTRO-WEB/TR2/>; (6) http://www.nao-rozhen.org/telescopes/fr_en.htm the 60cm Cassegrain has 26×26 arcmin field of view with the focal reducer; (7) Turcu et al. (2011); (8) <http://www.astrokolonica.sk/joomla15/index.php/sk/instruments.html>; (9) <http://belissima.aob.rs/>; (10) with 0.6× focal reducer; (11) Pribulla & Chochol (2003); (12) <http://oh.geof.unizg.hr/index.php/en/instruments/austro-croatian-telescope>; (13) <http://sln.oact.inaf.it/index.php/it/telescopio-91-cm/strumentazione/camera-ccd.html>; (14) <http://sln.oact.inaf.it/index.php/it/telescopio-apt2.html>; (15) Štefánik Observatory <http://www.observatory.cz/>; (16) http://www.tls-tautenburg.de/tls.d.php?category=test_d; (17) Mugrauer & Berthold (2010), STK - Schmidt Telescope Camera; (18) CTK - Cassegrain Telescope Camera; (19) Volkssternwarte Kirchheim; (20) private observatory at Herges-Hallenberg; (21) <http://homepages-fb.thm.de/jomo/t1t.htm>; (22) Lee et al. (2012).

cate the mechanism causing cyclic variations of the orbital period proposed by Applegate (1992).

The medium to high-resolution spectroscopy at the 2m telescope at the Rozhen observatory in Bulgaria¹⁷ will be performed for objects without any spectroscopy to infer the nature and spectral type of the components and to exclude systems with stellar third or multiple components.

Systematic CCD observations of the targets (Table 1) started at the Stará Lesná Observatory in February 2012 (see a sample of LCs obtained during the tests of the observing facilities at Stará Lesná in Fig. 1). The precision of

the data is good but still hardly approaching the theoretical limits given in the Table 1. The best error estimates of 4 primary minima determined from the preliminary reduction (differential photometry with respect to one comparison) of the CCD photometry of NY Vir (March 16, 24, and 26, 2012) range between 1.7 and 3.5 seconds while the theoretically estimated limit is 0.6 seconds. This results from the red noise in the data (no autoguider available), possible variability of the comparison star (GSC 4966-00559), and read-out overheads.

The (O-C) diagram of NY Vir using all published (Kilkenny et al., 1998, 2000; Hübscher, Paschke & Walker, 2006; Kilkenny, 2011; Zasche et al., 2011; Qian et al., 2012; Camurdan et al.,

¹⁷ http://www.nao-rozhen.org/index_bg.htm

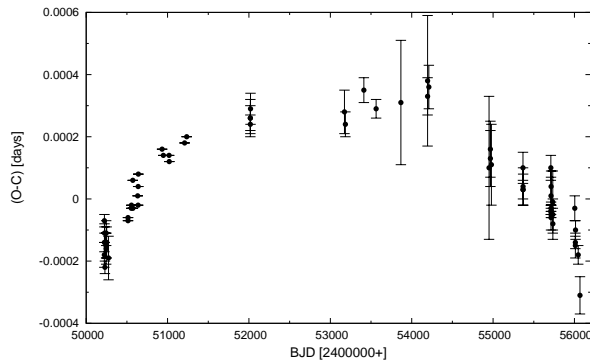


Fig. 2 *O-C* diagram for the sdB + M dwarf binary NY Vir. Six last points grouped around BJD 2 456 000 were determined from the CCD photometry obtained with the 60cm Cassegrain telescope at Stará Lesná (see Table 2). The *(O-C)* values were computed using linear ephemeris of Qian et al. (2012), $\text{Min I} = \text{BJD}2\,450\,223.362213(8) + 0.1010159673(2) \times E$.

2012) and 6 new minima timings is presented in Fig. 2. Our data are consistent with the overall period decrease in the system.

7 Conclusion

The presented project is aimed at the detection of circumbinary extrasolar planets and brown dwarfs using minima timing variability of carefully selected EBs. Unlike more widespread techniques (RV or transit searches) to detect extrasolar planets, the minima timing does not require high-end and costly astronomical instrumentation. Precise photometric observations of the brightest targets of our sample can be performed by well-equipped amateur astronomers. The chances to detect circumbinary bodies does not depend only on the precision of the individual timings but also on the number of participating institutions and devoted amateurs and number of targets monitored.

The theoretical estimates show that the timing technique enables to detect circumbinary planets down to Jupiter mass orbiting on a few-year orbits. The merit of an EB strongly depends on its brightness, depth, and width of the minima (see Eqn. 4), less on the mass of the underlying EB (Eqn. 5).

The observations within the project promise additional useful science such as: (i) the study of spot cycles in the RS CVn-like late-type binaries, detection of flares (see Pribulla et al., 2001), (ii) a more accurate characterization of recently discovered detached eclipsing binaries, (iii) detection of new low-mass EBs which is crucial to better define the empirical lower main sequence, (iv) determination of absolute parameters of the components (in the case that spectroscopic orbits are available), (v) detection of EBs with pulsating component(s), (vi) detection and characterization of multiple systems with two systems of eclipses, (vii) detection of new variable stars in the CCD fields covered, (viii) photometric detection of transits of substellar components across

the disks of the components of the eclipsing pair (see Doyle et al., 2011), (ix) detection of invisible massive components causing precession of the EB orbit and changes of the minima depth (see Mayer et al., 2004).

The LITE can always be regarded *only* as very good indication of a substellar body in the system. In nearby systems with a sufficiently close visual companion (e.g., CU Cnc, GK Boo) the LITE on a long-period orbit could be possibly checked by the differential astrometry of the visual pair.

Acknowledgements. This work has been funded by the VEGA 2/0094/11.

This study has made use of the SIMBAD database, operated at CDS, Strasbourg, France and NASA's Astrophysics Data System Bibliographic Services. PSz and TSz would like to thank the Hungarian OTKA Grant K76816. The work of the Bulgarian team (DK and DD) is partially supported by projects DO 02-362, DO 02-85 and DDVU 02/40-2010 of the Bulgarian National Science Fund. JWL acknowledge the support of Korea Astronomy and Space Science Institute (KASI) grant 2012-1-410-02. AF, GC, and AB gratefully acknowledge the Italian Ministero dell'Istruzione, Universit e Ricerca (MIUR). PD would like to thank the Slovak Research and Development Agency grant LPP-0024-09. GM and AN acknowledge Iuventus Plus grants IP2010 023070 and IP2011 031971. MZ would like to thank the project MUNI/A/0968/2009. PO, ML and AH would like to thank the project FWF: P22950-N16 with title: "Stellar signatures of mass expulsions in Radio and Optical wavelengths – Importance for stellar planetary interactions". MM acknowledge DFG for support in program MU2695/13-1. TP, MV, EK, and LH thank for the support to the project APVV-0158-11. MAVe acknowledges support by DLR under the project 50 OW 0204. MHMM thanks to grant Pest-C/CTM/LA0025/2011 (T-Portugal).

References

- Applegate, J.H. 1992, *ApJ* 385, 621
- Azzam, Y.A., Ali, G.B., Elnagahy, F. et al. 2010, in "Proceedings of the Third UN/ESA/NASA Workshop on the International Heliophysical Year 2007 and Basic Space Science", H.J. Haubold & A.M. Mathai (eds.), *Ap&SS proceedings*, Springer Verlag, p175
- Benest, D.: 2003, *A&A* 400, 1103
- van den Besselaar, E.J.M., Greimel, R., Morales-Rueda, L. et al.: 2007, *A&A* 466, 1031
- Beuermann, K., Hessman, F.V., Dreizler, S. et al.: 2010, *A&A* 521, L60
- Beuermann, K., Buhlmann, J., Diese, J. et al.: 2011, *A&A* 526, 53
- Broeg, Ch., Fern andez, M., Neuh user, R.: 2005, *AN* 326, 134
- Broucke, R.A.: 2001, *Celestial Mechanics and Dynamical Astronomy* 81, 321
-  akırlı,  ., İbano lu, C.: 2010, *MNRAS* 401, 1141
-  akırlı,  ., İbano lu, C., G ng r, C.: 2009, *NewA* 14, 496
-  amurdan, C.M., Zengin  amurdan, D., İbano lu, C.: 2012, *NewA* 17, 325
- Covino, E., Frasca, A., Alcal , J.M. et al.: 2004, *A&A* 427, 637
- Creevey, O.L., Benedict, G.F., Brown, T.M. et al.: 2005, *ApJ* 625, L127
- Deeg, H.J., Ocana, B., Kozhevnikov, V.P. et al.: 2008, *A&A* 480, 563
- Dimitrov, D.P., Kjurkchieva, D.P.: 2010, *MNRAS* 406, 2559
- Djura ević, G., Yılmaz, M., Ba t rk,  . et al. 2011, *A&A* 525, A66

- Doyle, R.L., Deeg, H.J., Jenkins, J.M. et al. 1998, in ASP Conf. Ser. 134, "Astrophysics of Variable Stars", R. Rebolo, E.L. Martin & M.R. Zapatero Osorio (eds.), p224
- Doyle, L.R., Carter, J.A., Fabrycky, D.C. et al.: 2011, *Science* 333, 1602
- Duquenois, A., Mayor, M.: 1991, *A&A* 248, 485
- Efron, B., Tibshirani, R.: 1993, "An Introduction to the Bootstrap", Boca Raton, FL: Chapman & Hall/CRC. ISBN 0412042312
- For, B.Q., Green, E.M., Fontaine, G. et al.: 2010, *ApJ* 708, 253
- Freudling, W., Romaniello, M., Patat, F. et al.: 2007, in ASP Conf. Ser. 364, "The Future of Photometric, Spectrophotometric and Polarimetric Standardization", C. Sterken (ed.), p113
- Gozdzewski, K., Nasiroglu, I., Slowikowska, A. et al. 2012, *MNRAS*, in press (2012arXiv1205.4164G)
- Hartman, J.D., Bakos, G.A., Noyes, R.W. et al.: 2011, *AJ* 141, 166
- Henden, A.A., Kaitchuck, R.H.: 1982, "Astronomical Photometry", Van Nostrand Reinhold comp.
- Hoffman, D.I., Harrison, T.E., Coughlin, J.L. et al.: 2008, *AJ* 136, 1067
- Hübscher, J., Paschke, A., Walker, F.: 2006, *IBVS* 5731
- Irwin, J.B.: 1959, *ApJ* 64, 149
- Irwin, J., Charbonnea, D., Berta, Z.K. et al.: 2009, *ApJ* 701, 1436
- Kilkenny, D.: 2011, *MNRAS* 412, 487
- Kilkenny, D., O'Donoghue, D., Koen, C. et al.: 1998, *MNRAS* 296, 329
- Kilkenny, D., Keuris, S., Marang, F. et al.: 2000, *The Observatory* 120, 48
- Konacki, M., Muterspaugh, M.W., Kulkarni, S.R., Helminiak, K.G.: 2009, *ApJ* 704, 513
- Konacki, M., Kozłowski, S., Sybilski, P. et al.: 2011, *American Astronomical Society, ESS meeting No. 2*,
- Kwee, K.K., van Woerden, H.: 1956, *Bull. of the Astronomical Institutes of the Nether.* 12, 327
- Kundra, E., Hric, L. 2011, *Ap&SS* 331, 121
- Law, N.M., Kraus, A.L., Street, R. et al.: 2012, submitted to *ApJ*, <http://arxiv.org/abs/1112.1701>
- Lee, J.W., Kim, C.H., Koch, R.H.: 2007, *MNRAS* 379, 1665
- Lee, J.W., Kim, S.L., Kim, Ch.H. et al.: 2009, *AJ* 137, 3181
- Lee, J.W., Youn, J.H., Kim, S.L. et al.: 2012, *AJ*, 143, 95
- López-Morales, M., Orosz, J.A., Shaw, J.S. et al.: 2006, 2006arXiv0610.225
- Malkov, O.Y., Oblak, E., Snegireva, E.A. Torra, J.: 2006, *A&A* 446, 785
- Maxted, P.F.L., Marsh, T.R., Morales-Rueda, L. et al.: 2004, *MNRAS* 355, 1143
- Mayer, P., Pribulla, T., Chochol, D.: 2004, *IBVS* 5563
- Morales, J.C., Ribas, I., Jordi, C. et al.: 2009, *ApJ* 691, 1400
- Moriwaki, K., Nakagawa, Y.A.: 2004, *ApJ* 609, 1065
- Mugrauer, M., Berthold, T.: 2010, *AN* 331, 449
- Muterspaugh, M.W., Konacki, M., Lane, B.F., Pfahl, E.: 2007, 2007arXiv0705.3072M
- Ofir, A.: 2008, *MNRAS* 387, 1597
- Ostensen, R.H., Oreiro, R., Hu, H. et al. 2008, in "Hot Subdwarf Stars and Related Objects", U. Heber et al. (eds.), ASP Conference Series, Vol. 392, 221
- Pakštie, E., Solheim, J.E.: 2003, *Baltic Astronomy*, 12, 221
- Parsons, S.G., Marsh, T.R., Copperwheat, C.M. et al. 2010, *MNRAS* 402, 2591
- Parsons, S.G., Marsh, T.R., Gansicke, B.T. et al.: 2011, *ApJ* 735, L30
- Pierens, A., Nelson, R.P.: 2008, *A&A* 483, 633
- Pilat-Lohinger, E., Dvorak, R.: 2002, *Celestial Mechanics and Dynamical Astronomy* 82, 143
- Pilat-Lohinger, E., Funk, B., Dvorak, R.: 2003, *A&A* 400, 1085
- Pojmanski, G.: 2002, *Acta Astronomica*, 52, 397
- Pojmanski, G.: 2003, *Acta Astronomica*, 53, 341
- Pojmanski, G., Maciejewski, G.: 2004a, *Acta Astronomica* 54, 153
- Pojmanski, G., Maciejewski, G.: 2004b, *Acta Astronomica* 55, 97
- Pojmanski, G., Pilecki, B., Szczygiel, D.: 2005, *Acta Astronomica* 55, 275
- Potter, S.B., Romero-Colmenero, E., Ramsay, G.: 2011, *MNRAS* 416, 2202
- Press, W.H., Teukolsky, S.A., Vetterling, W.T., Flannery, B.P.: 2007, "Numerical Recipes 3rd Edition: The Art of Scientific Computing", Cambridge University Press
- Pribulla, T., Chochol, D. 2003, *Baltic Astronomy*, 12, 555
- Pribulla, T., Baluđanský, D., Dubovský, P. et al.: 2008, *MNRAS* 390, 798
- Pribulla, T., Chochol, D., Heckert, P.A. et al.: 2001, *A&A* 371, 997
- Pribulla, T., Rucinski, S.M.: 2006, *AJ* 131, 2986
- Pribulla, T., Rucinski, S.M., Blake, R.M. et al.: 2009, *AJ* 137, 3655
- Qian, S.B., Liao, W.P., Zhu, L.Y., Dai, Z.B.: 2010, *ApJ* 708, 66
- Qian, S.B., Liu, L., Liao, W.P. et al.: 2011, *MNRAS* 414, L16
- Qian, S.B., Liu, L., Zhu L.Y. et al.: 2012, *MNRAS* 422, 24
- Quintana, E.V., Lissauer, J.J.: 2006, *Icarus* 185, 1
- Ribas, I.: 2003, *A&A* 398, 239
- Ribas, I.: 2006, in ASP Conf. Ser. 349, "Astrophysics of Variable Stars", C. Sterken & C. Aerts (eds.), p55
- Silvotti, R., Schuh, S., Janulis, R. et al.: 2007, *Nature* 449, 189S
- Tamuz, O., Mazeh, T., Zucker, S. 2005, *MNRAS* 356, 1466
- Terrell, D., Koff, R.A., Henden, A.A. et al. 2005, *IBVS* 5624
- Torres, G., Ribas, I.: 2002, *ApJ* 567, 1140
- Turcu, V., Pop, A., Marcu, A., Moldovan, D.: 2011, *Ap&SS* 331, 105
- Welsh, W.F., Orosz, S.A., Carter, J.A. et al.: 2012, *Nature* 481, 475
- Wils, P., Di Scala, G., Otero, S.A. 2007, *IBVS* 5800
- Wils, P., Lampens, P., Van Cauteren, P., Southworth, J.: 2010, *IBVS* 5940
- Windmiller, G., Orosz, J.A., Etzel, P.B.: 2010, *ApJ* 712, 1003
- Wolszczan, A., Frail, D.A.: 1992, *Nature* 355, 145
- Zhang, L., Zhang, X., Zhu, Z.: 2010, *NewA* 15, 362
- Zasche, P., Svoboda, P., Uhlář, R.: 2012, *A&A* 537, 109
- Zasche, P., Uhlář, R., Kučáková, H., Svoboda, P.: 2011, *IBVS* 6007